

Dynamic Beam-Based Random Access Scheme for M2M Communications in Massive MIMO Systems

Kan Zheng, *Senior Member, IEEE*, Haojun Yang, *Member, IEEE*, Xiong Xiong,
Jie Mei *Member, IEEE*, and Kuan Zhang, *Member, IEEE*

Abstract

Internet of things, supported by machine-to-machine (M2M) communications, is one of the most important applications for future 6th generation (6G) systems. A major challenge facing by 6G is enabling a massive number of M2M devices to access networks in a timely manner. Therefore, this paper exploits the spatial selectivity of massive multi-input multi-output (MIMO) to reduce the collision issue when massive M2M devices initiate random access simultaneously. In particular, a beam-based random access protocol is first proposed to make efficient use of the limited uplink resources for massive M2M devices. To address the non-uniform distribution of M2M devices in the space and time dimensions, an Markov decision process (MDP) problem with the objective of minimizing the average access delay is then formulated. Next, we present a dynamic beam-based access scheme based on the double deep Q network (DDQN) algorithm to solve the optimal policy. Finally, simulations are conducted to demonstrate the effectiveness of the proposed scheme including the model training and random access performance.

Index Terms

Internet of things (IoT), random access, machine-to-machine (M2M) communications, and reinforcement learning (RL).

I. INTRODUCTION

Recently, various types of applications in Internet of things (IoT) have rapidly grown, especially for industrial field. A high number of end devices are deployed, and adopt IoT networks to transmit sensing data and control information in a timely manner. To well support IoT applications, the 3GPP has developed machine-type communications (MTCs) and ultra-massive machine-type communications (umMTCs) as typical use cases in 5th generation (5G) and 6th generation (6G) networks [1], [2]. Consequently, the cellular-enabled IoT networks are receiving considerable attention from the industry and academia for operating diverse IoT applications.

The current mobile cellular networks, however, may not be able to meet the requirements of either MTCs or umMTCs, because they were originally designed to support human-type communications. In contrast to human-to-human (H2H) communications, machine-to-machine (M2M) communications typically involve a massive number of devices with low-data rate transmitting small payloads sporadically [3]. Moreover, MTC devices usually are not uniformly deployed across geographical areas, due to various IoT applications existing in networks. Based on the unique features and location distribution of MTC traffic, the current cellular networks need to be greatly improved to efficiently handle M2M communications. In general, M2M devices are first required to establish air interface connections in cellular networks before data transmission. The corresponding access requests are transmitted in an uncoordinated manner over the random access channels (RACHs). Once an MTC device has been granted to access, it is scheduled to use specific radio resources over which data transmission takes place in a deterministic manner. However, when a massive number of MTC devices are deployed in the networks, the RACHs with the existing access schemes become seriously overloaded result in heavy congestion. To this end, one of key issues is how to guarantee the timely access requirements of massive M2M devices.

Some recent advances have been conducted on dealing with the previous challenge [4], [5]. First of all, the number of M2M devices that initiate random access at the same time can be limited by a pre-defined access probability in access class barring (ACB), thereby reducing the risk of collision [6]–[10]. Then, by delaying the access time of the M2M devices with delay-insensitive applications, all random access requests can be scheduled into different time slots, which can relieve physical random access channel (PRACH) congestion [11]–[13]. Meanwhile, the base station can dynamically allocate radio resources to M2M devices based on the conditions

of PRACHs and network loads [14], [15]. Additionally, the base station can fully control random access by adjusting the paging timing of M2M devices [5]. A dedicated time slot of random access also can be assigned to reduce the interference on H2H communications [6], [16]. Finally, the code-expanded access is another good method [17]. For instance, in order to reduce preamble collision, a virtual preamble can be created by integrating the classical preamble and PRACH channel index [18]. Although the previous methods can help to reduce the congestion in the cellular mobile network, the issue concerning the massive number of M2M devices is still not solved effectively.

In recent years, massive multi-input multi-output (MIMO) has become one of the key techniques in 5G and 6G networks. The challenges of massive M2M devices accessing massive MIMO systems have been investigated. For example, an approximate message passing based grant-free scheme is proposed to jointly detect active users and estimate channel state information (CSI) [19]. Furthermore, a grant-free random access scheme is studied to detect active M2M devices and uplink messages without CSI estimation in one shot [20]. With the aid of the spatial multiplexing concept, multiple users and devices can use the same time-frequency resources simultaneously, thereby improving system throughput and spectral efficiency [21], [22]. However, few schemes have explored how to use the spatial characteristics of massive MIMO to solve the random access problem of massive M2M devices [23]. Intuitively, the base station with a large antenna array can generate a huge number of beams in different directions. Due to the high spatial resolution of beams, mutually isolated spatial areas in specific directions is feasible for the cellular network, which is more beneficial to let a certain beam only serve the devices within its corresponding area [24].

To address the access problem of massive M2M devices located at different geographic locations, this paper proposes a beam-based dynamic random access scheme based on massive MIMO technique. In particular, some M2M devices located in the coverage of a certain beam can be divided into the same group, and can use the same set of preambles and radio resources. To further improve the utilization efficiency, the same set of preambles and radio resources can also be reused by the M2M devices in the different beams. Owing to the spatial orthogonality of different beams, the mutual interference among the M2M devices in different groups is extremely small. Therefore, the collision problem can be effectively alleviated, when a massive number of M2M devices initiate the access simultaneously

The main contributions of this paper include:

- We propose a beam-based random access protocol for massive M2M devices. A group of beams with unequal beamwidth are applied to address the impact of the non-uniform distribution of M2M devices in space and time on random access process.
- Based on the Markov decision process (MDP), an optimization problem with the objective of minimizing the average access delay is formulated. To solve the optimal policy, we develop a dynamic beam-based random access scheme based on the double deep Q network (DDQN) algorithm.
- In order to demonstrate the effectiveness of the proposed scheme, the model training performance and random access performance are compared with other reference random access schemes by the simulation results.

The rest of this paper is organized as follows. In Section II, a typical scenario and model are first presented. Then, a beam-based random access protocol for M2M devices is described in detail. Next, a dynamic beam-based random access problem is formulated as MDP model in Section III. Based on the deep deterministic policy gradient (DDPG), Section IV proposes an algorithm to find the optimal policy. Moreover, simulations are carried out to demonstrate the performance of the proposed dynamic scheme in Section V. Finally, the conclusions are presented in Section VI.

II. SYSTEM MODEL AND RANDOM ACCESS PROTOCOL

A. Scenario Description

As shown in Fig. 1, N_g beams generated by a base station with massive MIMO are adopted to communicate with M2M devices located in the different areas. Furthermore, a set of N_p preambles are used for random access within a single beam, but might be reused between different beams. In general, the spatial distribution of M2M devices is usually not uniform and is also highly dynamic. This results in different arrival rates of random access both in space dimension and time dimension. For purposes of analysis, the coverage area of a base station is divided into N_s equal sectors. The M2M devices are uniformly distributed in a single sector, and their random access requests follow a Poisson distribution, where the arrival rates of access can be denoted as $\lambda_j, j \in \{1, 2, \dots, N_s\}$.

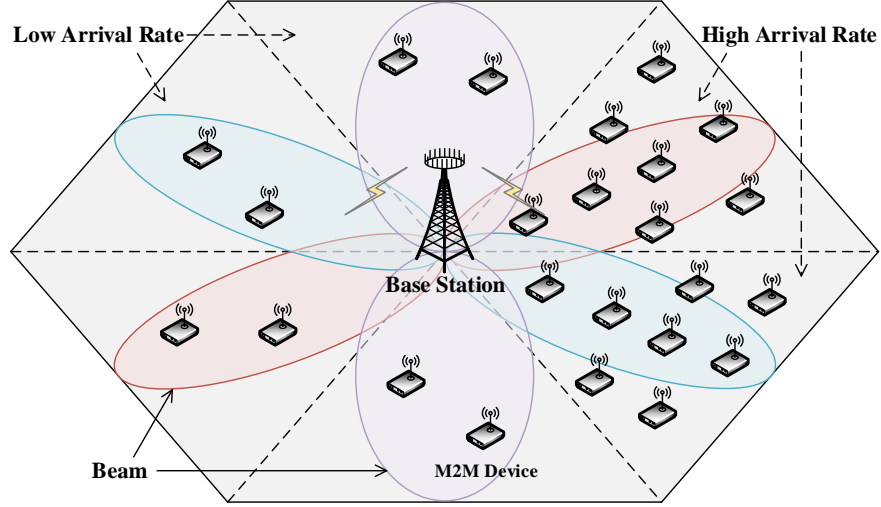


Fig. 1. Illustration of a base station with massive MIMO serving M2M devices.

B. Description of Beam-Based Random Access Protocol

In this paper, a beam-based random access protocol for massive M2M devices is proposed, and it mainly consists of the following four steps.

1) **Step 1 – Preamble Transmission:** Similarly with the regular random access protocol in Long-Term Evolution (LTE) systems, in our proposed protocol, a M2M device randomly selects and sends a preamble to the base station on the first available time slot of random access.

2) **Step 2 – Random Access Response:** After detecting the preamble sent by the M2M device, the base station sends the corresponding random access response (RAR) in the down-link, including the index of the detected preamble, the indicator of uplink resource and other information. When more than one M2M device send the same preamble, the base station will send the same RAR to them. However, it cannot tell whether a collision happens now, which has to be addressed in the subsequent steps.

3) **Step 3 – Connection Request:** Based on the received RAR, the M2M device sends an radio resource control (RRC) message to the base station. When the base station is equipped with massive MIMO, it can distinguish various RRC messages from the M2M devices located at different areas by multiple directional beams. Specifically, since most of the useful signals radiated by the antennas are concentrated within a beam, the beam has the remarkable spatial selectivity. Thus, the M2M devices located in the different beam coverage can be served separately, thereby reducing mutual interference. That is to say, for those M2M devices that send

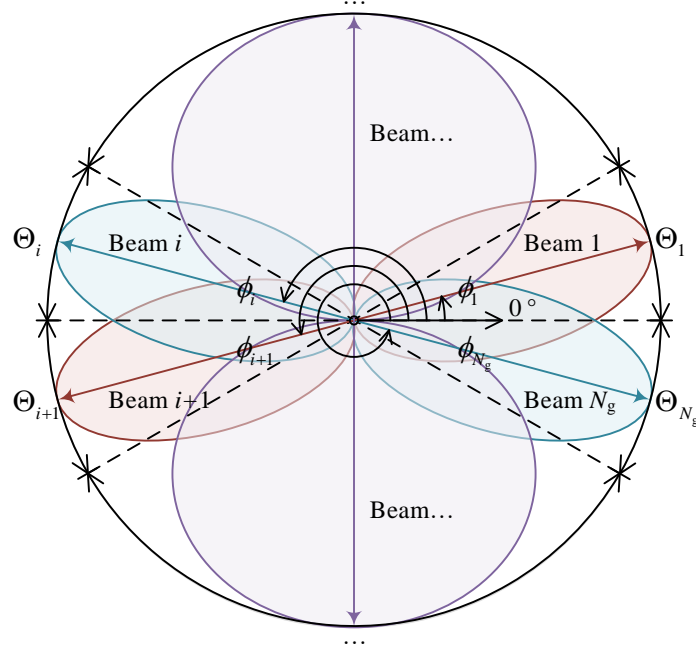


Fig. 2. Illustration of beam pattern with massive MIMO.

the same preamble and receive the same RAR, the base station can also distinguish the RRC messages through exploiting the spatial selectivity of different beams. Therefore, the beam-based random access scheme can efficiently improve the successful probability of random access.

4) **Step 4 – Contention Resolution:** After the base station successfully demodulates the RRC messages, it sends a contention resolution message back to the corresponding M2M device. Only the M2M device whose RRC message has been successfully demodulated can confirm the contention resolution message and complete the random access procedure, while other M2M devices fail to access.

C. Formulation of Beam-Based Random Access Protocol

In this section, we elaborate the proposed protocol mathematically. As shown in Fig. 2, each beam can be characterized by the maximum gain direction of ϕ_i and beamwidth of Θ_i . Generally, a beam is symmetric about its maximum gain direction, and most of its gain is concentrated within the beamwidth. In order to fully cover the service area of the base station, these beams need to be adjacent to each other with their beamwidth. In the other words, the maximum gain

Algorithm 1. Dynamic beam-based random access protocol.

Input:

- 1 The number of beams N_g ;
- 2 The number of preambles N_p ;
- 3 The arrival rates of access for N_s sectors, namely $\lambda_j, j \in \{1, 2, \dots, N_s\}$.

Procedure:

- 4 **Step 1 – Preamble Transmission:** The M2M devices randomly select and send preambles to the base station;
 - 5 **Step 2 – Random Access Response:** The base station first performs dynamic random access scheme as described in Algorithm 2, and then send the corresponding RAR;
 - 6 **Step 3 – Connection Request:** The M2M devices send the corresponding RRC messages to the base station;
 - 7 **Step 4 – Contention Resolution:** When the RRC messages are successfully decoded by the base station, i.e., the requirement in (5) is met, the M2M devices can receive the contention resolution message, and access to the network successfully.
 - 8 **if** *The M2M devices fail to access* **then**
 - 9 **Repeat** Step 1–4;
 - 10 **end**
-

direction and beamwidth of each beam should meet the following constraints, i.e.,

$$\left\{ \begin{array}{ll} \text{C1:} & \sum_{i=1}^{N_g} \Theta_i = 2\pi, \\ \text{C2:} & \phi_{(i \bmod N_g)+1} = \left[\phi_i + \right. \\ & \left. (\Theta_{(i \bmod N_g)+1} + \Theta_i) / 2 \right] \bmod 2\pi, \\ \text{C3:} & 0 \leq \phi_i, \Theta_i < 2\pi, i \in \{1, 2, \dots, N_g\}, \end{array} \right. \quad \begin{array}{l} (1a) \\ (1b) \\ (1c) \end{array}$$

where $\bmod(\cdot)$ represents the modulo operation.

Without loss of generality, let (θ_0, d_0) be the location of the interested M2M device in polar coordinate, where θ_0 and d_0 represent the angle and distance between the device and the base station, respectively. It is regarded as having successfully connected to the network only after

the base station demodulated the RRC message through the beam i^* . The serving beam i^* here refers to the one that the polar coordinate (θ_0, d_0) of the interested M2M device is converged within its bandwidth range, i.e.,

$$\begin{cases} \theta_{i^*}^L \leq \theta_0 < 2\pi \vee 0 \leq \theta_0 \leq \theta_{i^*}^H, & \theta_{i^*}^L > \theta_{i^*}^H, \\ \theta_{i^*}^L \leq \theta_0 \leq \theta_{i^*}^H, & \theta_{i^*}^L \leq \theta_{i^*}^H, \end{cases} \quad (2a)$$

$$\theta_{i^*}^L \leq \theta_0 \leq \theta_{i^*}^H, \quad \theta_{i^*}^L \leq \theta_{i^*}^H, \quad (2b)$$

where $\theta_{i^*}^L$ and $\theta_{i^*}^H$ are lower and upper boundaries of the serving beam i^* . Here we take the periodicity of the angle into account, i.e., $\theta_{i^*}^L = (\phi_{i^*} - \Theta_{i^*}/2) \bmod 2\pi$, $\theta_{i^*}^H = (\phi_{i^*} + \Theta_{i^*}/2) \bmod 2\pi$.

For the interested M2M device, the signals with RRC messages sent by the other N_I M2M devices served by those beams different from the beam i^* are regarded as interference, because the same uplink radio resource is used. The received power of the interference at the serving beam i^* for the interested device can be expressed as (in dBm)

$$I_{i^*} = 10 \log_{10} \left[\sum_{q=1}^{N_I} 10^{R_{i^*}(\theta_q, d_q)/10} \right], q \in \{1, 2, \dots, N_I\}. \quad (3)$$

Accordingly, at the i -th beam of the base station, the received power of the signal with the RRC message are generally calculated by (in dBm)

$$\begin{aligned} R_i(\theta, d) = & P_t + G_t + G_r + 20 \log_{10}(f_i(\theta)) \\ & - \text{PL}(d) + \chi, i \in \{1, 2, \dots, N_g\}, \end{aligned} \quad (4)$$

where P_t represents the transmit power of the M2M device, while G_t and G_r are the gains of transmit and receive antennas, respectively. $\text{PL}(d)$ is the path loss between the M2M device and base station, and χ is the shadow fading obeying a Gaussian distribution with zero mean and variance σ^2 . Lastly, $f_i(\theta)$ represents the gain of the i -th beam in the direction θ , and Appendix A gives the calculation of the gain.

Finally, when the power difference in logarithmic value between the RRC message and the interference is larger than the required demodulation threshold Γ , the base station can successfully decode the RRC message of the interested M2M device, i.e.,

$$R_{i^*}(\theta_0, d_0) - I_{i^*} > \Gamma. \quad (5)$$

To sum up, the dynamic beam-based random access protocol is proposed in Algorithm 1. In the next section, we mainly focus on the study of the dynamic random access part.

TABLE I
EXAMPLE OF ACTION SPACE

Action	Beam 1		Beam 2		Beam 3		Beam 4		Beam 5		Beam 6	
	ϕ_1	Θ_1	ϕ_2	Θ_2	ϕ_3	Θ_3	ϕ_4	Θ_4	ϕ_5	Θ_5	ϕ_6	Θ_6
a_1	$\frac{1}{12}\pi$	$\frac{1}{6}\pi$	$\frac{1}{2}\pi$	$\frac{2}{3}\pi$	$\frac{11}{12}\pi$	$\frac{1}{6}\pi$	$\frac{13}{12}\pi$	$\frac{1}{6}\pi$	$\frac{3}{2}\pi$	$\frac{2}{3}\pi$	$\frac{23}{12}\pi$	$\frac{1}{6}\pi$
a_2	$\frac{5}{12}\pi$	$\frac{1}{6}\pi$	$\frac{5}{6}\pi$	$\frac{2}{3}\pi$	$\frac{5}{4}\pi$	$\frac{1}{6}\pi$	$\frac{17}{12}\pi$	$\frac{1}{2}\pi$	$\frac{11}{6}\pi$	$\frac{2}{3}\pi$	$\frac{1}{4}\pi$	$\frac{1}{6}\pi$
a_3	$\frac{3}{4}\pi$	$\frac{1}{6}\pi$	$\frac{7}{6}\pi$	$\frac{2}{3}\pi$	$\frac{19}{12}\pi$	$\frac{1}{6}\pi$	$\frac{7}{4}\pi$	$\frac{1}{2}\pi$	$\frac{13}{6}\pi$	$\frac{2}{3}\pi$	$\frac{7}{12}\pi$	$\frac{1}{6}\pi$

III. PROBLEM FORMULATION OF DYNAMIC BEAM-BASED RANDOM ACCESS

According to the proposed beam-based random access process, the base station can *dynamically* adjust the direction and beamwidth of the beam based on the non-uniform distribution of M2M devices. Thus, the number of devices located in the coverage of different beams can be effectively balanced, thereby alleviating the collision in random access process. In this section, the *dynamic* random access problem is formulated as a MDP model, and its state, action, and revenue are defined as follows.

A. State

The state $s \in \mathcal{S}$ includes the number of M2M devices that initiate random access in each sector area, i.e.,

$$\mathcal{S} = \{s \mid s = (n_1, n_2, \dots, n_{N_s})\}, \quad (6)$$

where $n_j, j \in \{1, 2, \dots, N_s\}$ represents the number of M2M devices accessing in the j -th sector.

B. Action

The action $a \in \mathcal{A}$ defines how the base station to adjust the direction and width of the beams, which can be expressed by

$$\mathcal{A} = \{a \mid a = (\phi_1, \Theta_1, \phi_2, \Theta_2, \dots, \phi_{N_g}, \Theta_{N_g})\}, \quad (7)$$

where ϕ_i and $\Theta_i, i \in \{1, 2, \dots, N_g\}$ are the maximum gain direction and beamwidth of the i -th beam, respectively. It is noted that the direction and beamwidth of each beam strictly follow the

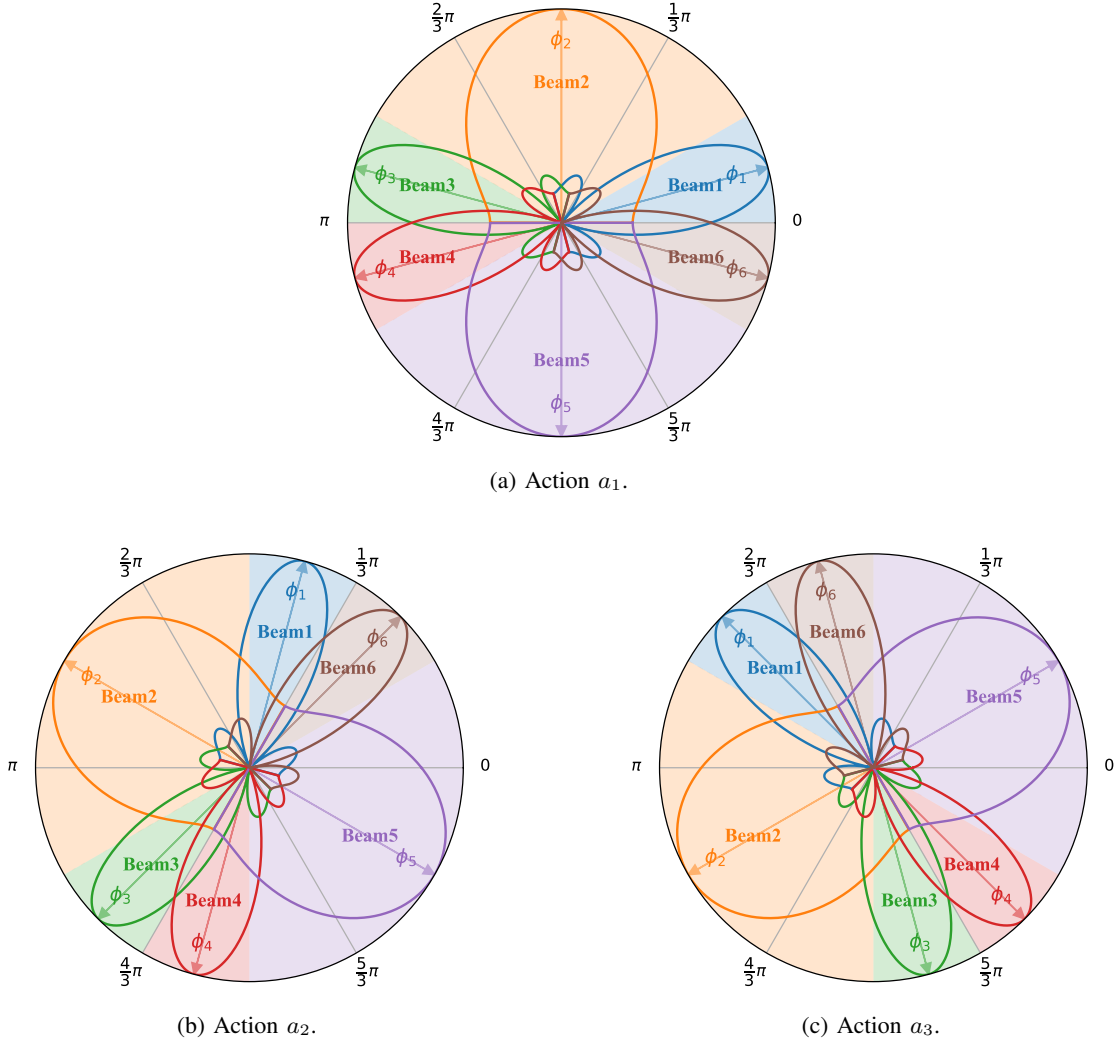


Fig. 3. Example of dynamic beam-based random access.

requirements in (1). For the simplicity of illustration, the action only includes several typical selections with the given number of beams, i.e.,

$$\mathcal{A} = \{a_1, a_2, \dots, a_{|\mathcal{A}|}\}, \quad (8)$$

where $|\mathcal{A}|$ represents the size of the action space, and $a_i, i \in \{1, 2, \dots, |\mathcal{A}|\}$ are pre-defined typical actions¹. Assume that the number of beams N_g is equal to 6, and the action space \mathcal{A} contains 3 typical actions as shown in Table I, then the beam gain of each action is given in Fig. 3.

¹Here a typical group of beams with unequal beamwidth is presented only as an illustration of beam-based access schemes, since the beam design is beyond the scope of this paper.

Remark 1: When one action is selected, e.g., a_1 , the signal gains received by the base station from different directions may vary considerably, since multiple beams have different beamwidths. In other words, the base station have better signal gain but less coverage using one of beams, and vice versa. The beams used in actions a_2 and a_3 are obtained by rotating the beams of action a_1 counterclockwise by $\pi/3$ and $2\pi/3$, respectively. Therefore, the beams corresponding to different actions may better serve M2M devices located in various directions.

C. State Transition

In this paper, the state transition is simply expressed as $s \xrightarrow{a} s'$, which means that the current state s transfers to the new state s' after executing action a . To better reflect the dynamic feature of random access process, the MDP model of this paper adopts *episodic task* based state transition process, including a series of relatively independent *episodes* [25]. Each episode contains the following state transition steps, i.e.,

1) **Phase 1:** At the beginning of each episode, the M2M devices in each sector initiate the random access process at the slot $t = 0$ with the given arrival rates λ_j , $j \in \{1, 2, \dots, N_s\}$. Correspondingly, the initial state is represented by $s = S_{(0)}$.

2) **Phase 2:** Based on the number of devices, the base station adjusts the direction and beamwidth according to the policy π , namely $a = \pi(s)$. Then, the base station operates the proposed beam-based random access protocol as described in Section II. Additionally, the M2M devices that fail to access will continue to initiate an access request at the next slot t' . At this point, the state of the model is updated as $s' = S_{(t')}$.

3) **Phase 3:** If most of the M2M devices initiating the random access process in the initial state $S_{(0)}$ have successfully connected the network before updating the new state $S_{(t')}$, the current episode terminates. This also means that only a few M2M devices fail to access the network, i.e., $\sum_{j=1}^{N_s} n'_j \leq n_T$, where n_T is the performance threshold. Otherwise, update the slot $t \leftarrow t'$ and state $s \leftarrow s'$, and repeat the **Phase 2** of the state transition.

Finally, when an episode is terminated, the model transfers to a new independent episode and performs **Phase 1–3** as described above.

D. Reward

The reward $r(s, a)$ is a real-valued function of the state s and the action a , reflecting the benefits and costs of the current instantaneous decision $a = \pi(s)$. Therefore, the reward definition

has to be consistent with the optimization objective. Since the model of this paper relies on instantaneous value rather than statistical one, the successful probability of access can not be directly used as the optimization objective. To this end, an alternative optimization is required. Generally, the policy π can be regarded as working well, if the access requests of all M2M devices can be performed successfully and quickly. Meanwhile, it also implies that this policy π can improve the successful probability of access. Therefore, we choose the access delay as the performance metric of random access rather than the probability. In conclusion, the goal of the model is to minimize the average delay of random access.

According to the above state transition process, when the model in a certain episode transfers from the current state $s = (n_1, n_2, \dots, n_{N_s})$ to a new state $s' = (n'_1, n'_2, \dots, n'_{N_s})$ by taking the action a , the number of M2M devices that fail to access the network can be expressed by

$$\hat{r}(s, a) = \sum_{j=1}^{N_s} n'_j. \quad (9)$$

Since these M2M devices may try to access again in the new state s' , each of them spends one more time slot compared with those M2M devices that have successfully accessed in the state s . Thus, $\hat{r}(s, a)$ can be the proxy of the “access delay” during the state transition $s \xrightarrow{a} s'$, it also is the number of time slots used for random access. By summing up $\hat{r}(s, a)$ of all states in an episode, the “total access delay” of M2M devices can be obtained by

$$\hat{G}_\tau = \sum_{t=0}^{T_\tau} \hat{r}(S_{(t)}, A_{(t)}) = \sum_{m=1}^{|S_{(0)}|} \sum_{t=0}^{T_\tau} \mathbf{1}_{m \notin S_{(t)}}, \quad (10)$$

where T_τ represents the termination moment of the episode τ , while $S_{(t)}$ and $A_{(t)}$ represent the state and action at the time slot t of random access, respectively. $|S_{(0)}|$ is the number of M2M devices that initiate random access requests in the initial state, namely $|S_{(0)}| = \sum_{j=1}^{N_s} n_j$. Let $\mathbf{1}_{m \notin S_{(t)}}$ indicate whether the m -th M2M device in the initial state has successfully accessed the network at the time slot t . If the M2M device has not yet connected to the network, i.e., $\mathbf{1}_{m \notin S_{(t)}} = 1$; otherwise, $\mathbf{1}_{m \notin S_{(t)}} = 0$. Thus, the access delay of the m -th M2M device can be calculated by $\sum_{t=0}^{T_\tau} \mathbf{1}_{m \notin S_{(t)}}$. Next, the average access delay can be given by

$$\bar{G}_\tau = \hat{G}_\tau / (|S_{(0)}| - \hat{r}(S_{(T_\tau)}, A_{(T_\tau)})), \quad (11)$$

where $\hat{r}(S_{(T_\tau)}, A_{(T_\tau)}) < n_T$.

Based on the above definition, the reward finally can be expressed by

$$r(s, a) = -\hat{r}(s, a). \quad (12)$$

Here, a negative sign is adopted, this is because the reward definition of MDP must satisfy the following assumption, i.e., the larger the reward value, the better the action. Accordingly, the cumulative reward from time slot t to the termination moment of episode τ can be given by

$$\begin{aligned} G_{\tau(t)} &= \sum_{k=t}^{T_\tau} \gamma^{k-t} r(S_{(k)}, A_{(k)}) \\ &= - \sum_{k=t}^{T_\tau} \gamma^{k-t} \hat{r}(S_{(k)}, A_{(k)}), \end{aligned} \quad (13)$$

where γ is the so-called discount factor. Since the formulated model in this section is based on the episodic task, then $\gamma = 1$. In conclusion, maximizing the the expected cumulative reward $\mathbb{E}_\pi[G_{\tau(t)}]$ is equivalent to minimizing the average “access delay” of M2M devices, which is consistent with our original optimization goal.

IV. DYNAMIC RANDOM ACCESS SCHEME WITH DDQN

To find the optimal policy π^* for maximizing the expected cumulative reward $\mathbb{E}_{\pi^*}[G_{\tau(t)}]$, we propose an dynamic random access scheme based on the DDQN algorithm to solve the MDP model. The DDQN algorithm is a value-based reinforcement learning technique that utilizes a neural network to approximate the value function $Q_\pi(s, a)$, i.e.,

$$\begin{aligned} Q(s, a; \boldsymbol{\theta}) &\approx Q_\pi(s, a) \\ &= \mathbb{E}_\pi [G_{\tau(t)} \mid S_{(t)} = s, A_{(t)} = a] \\ &= \mathbb{E}_\pi \left[\sum_{k=t}^{\infty} \gamma^{k-t} r(S_{(k)}, A_{(k)}) \mid S_{(t)} = s, A_{(t)} = a \right], \end{aligned} \quad (14)$$

where $\boldsymbol{\theta}$ is the weight parameter of the neural network $Q(s, a; \boldsymbol{\theta})$. $Q(s, a; \boldsymbol{\theta})$ is also known as the ***prediction network***, whose input is a N_s -dimension vector representing the current state s and output is a $|\mathcal{A}|$ -dimension vector representing the action value corresponding to each action a . Then, by using the action value function, the corresponding policy can be directly obtained by $\pi(s) = \operatorname{argmax}_{a \in \mathcal{A}} Q_\pi(s, a) \approx \operatorname{argmax}_{a \in \mathcal{A}} Q(s, a; \boldsymbol{\theta})$.

In order to estimate the action value function accurately, we have to use another ***target network***, namely $Q(s, a; \boldsymbol{\theta}^-)$, which has the same structure with the prediction network [26]. Then, the

Algorithm 2. Dynamic random access scheme for non-uniform grouping case based on DDQN.

Input:

- 1 Initialize the prediction network $Q(s, a; \theta)$ with random weights θ ;
- 2 Initialize the target network $Q(s, a; \theta^-)$ with weights $\theta^- = \theta$;
- 3 Initialize the replay memory D ;
- 4 Initialize $\varepsilon = 1$.

Procedure:

```

5 for  $\tau \leftarrow 1, \dots, \infty$  do
6   Initialize the state  $s = S_{(0)}$  according to the arrival rate  $\lambda_j, j \in \{1, 2, \dots, N_s\}$ ;
7   for  $t \leftarrow 1, \dots, \infty$  do
8     Generate a random number  $p, 0 < p \leq 1$  ;                                /*  $\varepsilon$ -greedy */
9      $a \leftarrow \begin{cases} a \in_R \mathcal{A} & 0 \leq p < \varepsilon \\ \operatorname{argmax}_{a \in \mathcal{A}} Q(s, a; \theta) & \varepsilon \leq p < 1 \end{cases}$  ;
10    Take the action  $a$  and perform state transition  $s \xrightarrow{a, r(s, a)} s'$ ;
11    Save the experience  $e \leftarrow (s, a, r(s, a), s')$  into the replay memory  $D$ ;
12    Random sample a batch of experiences  $\tilde{D}$  from  $D$ ;
13    Calculate  $L(\theta)$  ;                                /* according to (15) */
14    Update weights  $\theta$  by optimizer;
15    if  $\varepsilon > \varepsilon_{\min}$  then                                /* exponential decay of  $\varepsilon$  */
16      |  $\varepsilon \leftarrow \varepsilon \cdot \varepsilon_{\text{decay}}$ ;
17    end
18    if  $t \bmod n_\theta = 0$  then                                /* every  $n_\theta$  steps */
19      |  $\theta^- \leftarrow \theta$ ;
20    end
21    if  $\hat{r}(s, a) \leq n_T$  then                                /* episode end  $T_\tau = t$  */
22      | break;
23    end
24     $s \leftarrow s'$ ;
25  end
26 end

```

Output: Obtain the optimal policy π^* based on (16).

mean squared error (MSE) function can be defined by

$$L(\theta) = \frac{1}{|\tilde{D}|} \sum_{e \in \tilde{D}} \left[\left(r(s, a) - Q(s, a; \theta) \right)^2 \right]$$

TABLE II
MAIN PARAMETERS IN SIMULATIONS

Parameter	Description	Value
MDP Model Related Parameters		
λ	Total arrival rate of M2M devices	150, 300
ρ	Distribution ratio	2, 5, 20
d	Distance between M2M devices and base station	0 - 10 km
N_p	Number of the preambles	48
N_g	Number of beams	6
P_t	Transmit power of M2M device	23 dBm
G_t	Transmit antenna gain of M2M device	0 dBi
G_r	Receive antenna gain of base station	18 dBi
σ	Standard variance of shadowing	8 dB
$PL(d)$	Path loss	$120.9 + 37.6 \log_{10}(d)$
Γ	Demodulation threshold	-110 dBm
DDQN Algorithm Related Parameters		
ε_{\min}	Minimum ε	0.01
$\varepsilon_{\text{decay}}$	ε Exponential decay	0.99
α	Learning rate	0.001
$ D $	Size of replay memory D	1200
$ \tilde{D} $	Number of samples per batch	64
n_{θ}	Weight update period of the target networks θ^-	16

$$+ \gamma Q(s', \arg\max_{a'} Q(s', a'; \theta); \theta^-)^2 \Big], \quad (15)$$

where $e = (s, a, r(s, a), s')$ is an experience sample including the state s , action a , new state s' and the resulting reward $r(s, a)$ in the state transition process of $s \xrightarrow{a, r(s, a)} s'$. \tilde{D} is a set of $|\tilde{D}|$ experiences, which are selected from the replay memory D with a first-in first-out (FIFO) queue. The DDQN algorithm updates the weight parameters of the neural network iteratively with the objective of minimizing the loss function $L(\theta)$ until the optimal action value function

is estimated, i.e., $Q(s, a; \theta^*) \approx Q_{\pi^*}(s, a)$. Afterwards, the optimal policy can be written as

$$\begin{aligned}\pi^*(s) &= \operatorname{argmax}_{a \in \mathcal{A}} Q_{\pi^*}(s, a) \\ &\approx \operatorname{argmax}_{a \in \mathcal{A}} Q(s, a; \theta^*).\end{aligned}\quad (16)$$

Algorithm 2 proposes a dynamic random access scheme for non-uniform grouping case based on DDQN. First of all, the related model parameters including the so-called prediction network, target network, and replay memory are initialized. Then, the iteration of a episode is carried out. At the beginning of each episode, the initial state $s = S_{(0)}$ is generated according to the arrival rates of access in each sector, i.e., $\lambda_j, j \in \{1, 2, \dots, N_s\}$. Subsequently, during each episode, the action a is selected based on the ε -greedy rule in the iteration of each access slot. In particular, the greedy policy is selected with the probability of $1 - \varepsilon$, while a random action is chosen with the probability ε . The ε decays exponentially with the parameter of $\varepsilon_{\text{decay}}$ at each iteration until it decays to the minimum value of ε_{\min} . The ε -greedy rule can efficiently prevent the algorithm from falling into the local optimal solution. Next, the algorithm executes the action a and performs the state transition. Meanwhile, the generated experience e are saved in the replay memory D . Finally, a batch of \tilde{D} experiences are randomly selected from the replay memory D to calculate the loss function $L(\theta)$, and the weight parameter θ of the prediction network is updated. It is noticed that only after n_θ iterations, the weight parameter θ^- of the target network is updated with the weight parameter θ of the prediction network, namely $\theta^- \leftarrow \theta$. When the algorithm converges, the optimal action value function $Q(s, a; \theta^*) \approx Q_{\pi^*}(s, a)$ is obtained as well as the optimal policy $\pi^*(s) \approx \operatorname{argmax}_{a \in \mathcal{A}} Q(s, a; \theta^*)$.

V. SIMULATION RESULTS AND ANALYSIS

A. Simulation Configuration

In the simulations, a base station with massive MIMO is divided into $N_s = 6$ sectors. The sectors are bounded by the directions of $[(j-1)\pi/3 - \pi/6, (j-1)\pi/3 + \pi/6], j \in \{1, 2, \dots, N_s\}$. The distance between the M2M devices and the base station varies randomly from 0 to 10 km. Moreover, the base station generates $N_g = 6$ beams, and adjusts the direction and width of the beams according to the action space \mathcal{A} as shown in Table I. To reflect the non-uniform feature of device distribution, one of sectors is set as the high-density area with the high arrival rate of access, such as $\lambda_1 = \lambda_{\text{high}}$, while other sectors are set with $\lambda_j = \lambda_{\text{low}}, j = 2, 3, \dots, N_s$. The total arrival rate is defined as $\lambda = \sum_{j=1}^{N_s} \lambda_j$. Finally, we also define a distribution ratio between

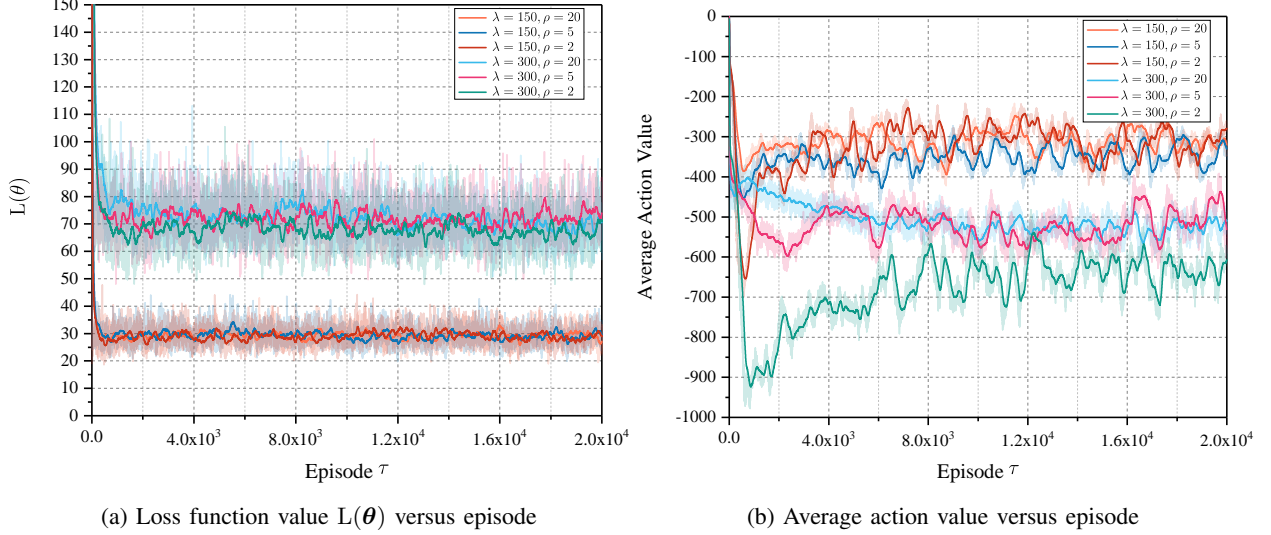


Fig. 4. Training performance of the proposed DDQN-based dynamic random access algorithm.

the high-density and low-density sectors as $\rho = \frac{\lambda_{\text{high}}}{(N_s - 1)\lambda_{\text{low}}}$ to evaluate the performance under various arrival rate. The main parameters of simulations are shown in Table II.

In the DDQN algorithm, both the prediction and the target networks use a two-layer fully connected neural network, in which each fully connected layer contains 64 neurons with the rectified linear unit (ReLU) activation function. The size of the replay memory $|D|$ is set to 1200. During each iteration, the algorithm selects 64 experiences per batch from the replay memory to calculate the loss function $L(\theta)$. In addition, the Adam optimizer with a learning rate of $\alpha = 0.001$ is applied to update the weight parameters θ of the prediction network. Finally, the parameters of the ε -greedy rule are set as $\varepsilon_{\min} = 0.01$ and $\varepsilon_{\text{decay}} = 0.99$, respectively. The weight update period of the target network θ^- is set as $n_\theta = 16$.

B. Performance Analysis

1) *Training Performance:* Fig. 4 shows the training performance of the proposed DDQN-based scheme after iterating 2×10^4 episodes in terms of the loss function and average action value. All solid lines represent the results after exponential moving average (EMA) processing with a weight of 0.99, while the original data is given in the shadow parts. The values of loss function under different arrival rates and distribution ratios are first presented in Fig. 4(a). Each curve shows a rapid downward trend during the first 10^3 episodes, and then is stabilized within a certain range. Particularly, the loss function value in the case of $\lambda = 300$ ends up fluctuating

TABLE III
AVERAGE ACCESS DELAY OF M2M DEVICES

Case	Static-BE	Random-BU	DDQN-BU	
	Average Value (Time slots)	Average Value (Time slots)	Average Value (Time slots)	Gain ¹
$\lambda = 150, \rho = 2$	3.72	3.56	3.42	4.1%
$\lambda = 150, \rho = 5$	4.01	3.94	3.53	10.4%
$\lambda = 150, \rho = 20$	4.29	4.28	3.66	14.7%
$\lambda = 300, \rho = 2$	4.66	4.65	4.15	10.7%
$\lambda = 300, \rho = 5$	5.24	5.32	4.44	16.6%
$\lambda = 300, \rho = 20$	5.96	6.24	4.75	23.9%

¹ The gain is defined as the average access delay of the **DDQN-BU** scheme divided by that of the **Static-BE** scheme.

between 60 - 80, while the loss function value under $\lambda = 150$ remains stable at about 30. After about the 2×10^3 episode, each loss function almost converges.

Subsequently, Fig. 4(b) gives the performance of average action value. Here the average action value refers to the average output of the prediction network in each episode, i.e., $\frac{1}{T_\tau \cdot |\mathcal{A}|} \sum_{t=1}^{T_\tau} \sum_{a \in \mathcal{A}} Q(S_{(t)}, S_{(t)}; \theta)$. Due to the different trajectories of state transition, the instantaneous action value is not comparable, and it cannot accurately reflect the convergence of the algorithm. Thus, instead of the instantaneous action value, the average one is chosen as the performance metric.

In the first 10^3 episodes of Fig. 4(b), each curve starts at 0 and shows a rapid downward trend. This is because the weight parameters of the prediction network are initialized with the standard *Glorot*, resulting in a small output value at the beginning of the training. Then, as the weight parameters are updated rapidly during the training progress, the average action value of the prediction network changes dynamically. After the 10^3 episodes, the curves under various λ show different trends. Specifically, in the case of $\lambda = 150$, three curves first rise slowly and then fluctuate between -250 and -400 . On the other hand, in the case of $\lambda = 300$, the curves with $\rho = 20$ or 5 still decline slowly, and gradually stabilize at around -500 . Furthermore, when $\lambda = 300$ and $\rho = 2$, the corresponding curve eventually stabilizes between -600 and -700 . Lastly, all of them almost reach a state of convergence after 10^4 episodes. In addition, it is noted that the average action value in the case of $\lambda = 300$ is much lower than that of $\lambda = 150$. This is

because the larger arrival rate λ , the greater chance of collision, which leads to a larger access delay and a lower action value. According to Fig. 4, it is evident that the proposed scheme with the DDQN algorithm becomes convergent fast and steadily.

2) *Delay Performance*: The proposed scheme based on multiple beams with unequal beamwidth (hereinafter referred to as **DDQN-BU**) is compared with the following random access schemes, i.e.,

- Static scheme based on multiple beams with equal beamwidth (**Static-BE**): In this scheme, all beams have the equal beamwidth, i.e., $\Theta_i = 2\pi/N_g$. Thus, there is no need to make selection during the random access [23].
- Random scheme based on multiple beams with unequal beamwidth (**Random-BU**): This scheme randomly selects one of the beams in Fig. 3 to serve all M2M devices, regardless of their spatial distribution.

Table III gives the average “access delay” when different random access schemes are applied under various arrival rates λ and distribution ratios ρ . It can be seen that the **DDQN-BU** scheme has the lower average access delay than others in all cases. At the same time, its relative gain to **Static-BE** scheme increases with the higher arrival rate and the larger distribution ratio. For example, in the case of $\lambda = 300$ and $\rho = 20$, the **DDQN-BU** scheme has the lowest average access delay of 4.75 slots, while the average access delay of the **Static-BE** scheme and **Random-BU** scheme are 5.96 and 6.24 slots, respectively. Therefore, the **DDQN-BU** scheme allows M2M devices to access the network faster by dynamically adjusting the beam direction and beamwidth, and owns optimal access performance.

When the distribution ratio ρ is first fixed, the average access delay of each scheme becomes larger with the increase of the arrival rate λ . We can further find that the gain of the **DDQN-BU** scheme compared with the **Static-BE** scheme also become more intuitive with the increase of the arrival rate λ . For example, at $\rho = 20$, the gain of **DDQN-BU** at $\lambda = 150$ and $\lambda = 300$ are 14.7% and 23.9%, respectively. This shows that the larger arrival rate λ is, the more intuitive optimization effect of the **DDQN-BU** scheme on the access performance achieves.

Next, we fix the arrival rate λ but increase the distribution ratio ρ . The average access delay of each scheme increases when the non-uniform distribution of devices becomes stronger, namely the larger ρ . This phenomenon is expected because M2M devices collide more frequently as the number of devices increases within a given sector, and thus the average access delay eventually rises. More importantly, the gain of the **DDQN-BU** scheme also becomes larger with the increase

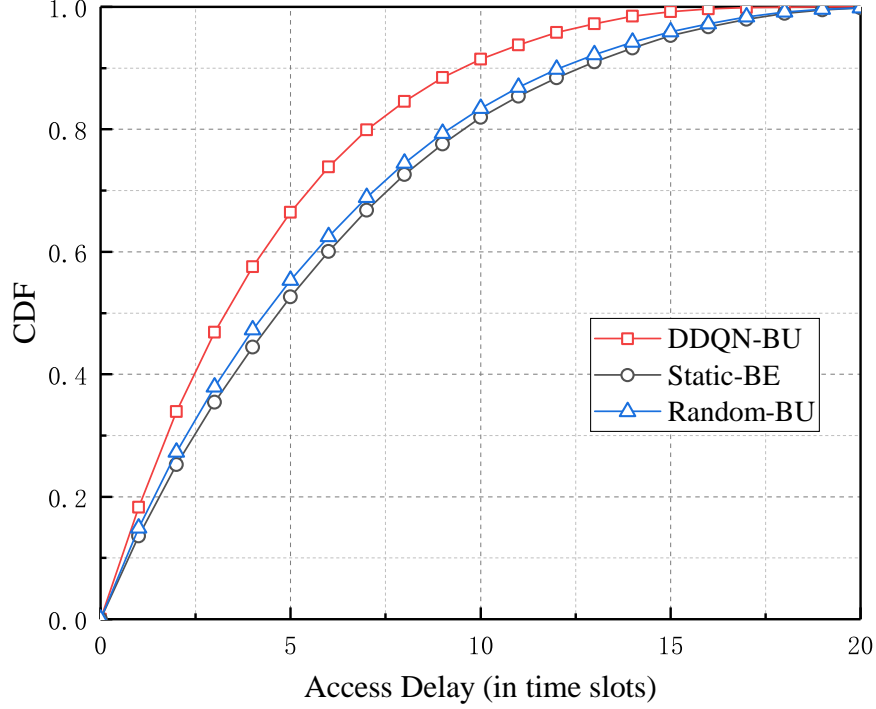


Fig. 5. CDF performance of access delay under different access schemes with $\lambda = 300$ and $\rho = 20$.

of the distribution ratio ρ . For example, at $\lambda = 150$, the gain improvements are 4.1%, 10.4% and 14.7% for $\rho = 2$, $\rho = 5$ and $\rho = 20$, respectively. This shows that the stronger non-uniform distribution, the more intuitive optimization effect of the **DDQN-BU** scheme on access performance. Compared with the reference schemes, the **DDQN-BU** scheme can better handle the access problem in the case of non-uniform distribution of M2M devices.

Finally, we further analyze the cumulative distribution function (CDF) performance of access delay. The CDF curves of access delay have the same trend under different arrival rates λ and distribution ratios ρ , thus here only the case of $\lambda = 300$ and $\rho = 20$ is taken as an example for the sake of analysis. As shown in Fig. 5, when the access delay is small, all curves increase rapidly, such an increase becomes slower as the access delay becomes larger. It means that most M2M devices have a low access delay, and only a few devices have a high access delay. For example, when the **DDQN-BU** scheme is adopted, about 66.4%, 91.5% and 99.2% of M2M devices access the network successfully within 5, 10 and 15 time slots, respectively. Furthermore, the CDF curve of the **DDQN-BU** scheme rises the fastest among all ones. This shows that the **DDQN-BU** scheme dynamically adjusts the beam direction and beamwidth according to the

distribution of devices, which can efficiently reduce the access delay and improve the overall access performance.

VI. CONCLUSION

Many IoT applications have the non-uniform distribution of devices in the space dimension, and the dynamic service arrival rate in the time dimension. As a result, this paper proposed a beam-based dynamic random access scheme in massive MIMO systems. Specifically, the base station can dynamically adjust a group of beams with different bandwidths based on the distribution of devices, which can efficiently balance the number of M2M devices served by different beams, reducing collisions during the access process. We also formulated this dynamic problem as a MDP model, and proposed a dynamic beam-based random access scheme based on the DDQN algorithm to obtain the optimal solution. Lastly, the performance of the proposed scheme were validated by simulations. The proposed scheme were proved to converge rapidly and stably. After the model is converged, the optimal policy can be determined by using the trained prediction neural network. The simulation results show that the proposed scheme performs much better than the other two reference schemes in terms of the average access delay.

APPENDIX A

CALCULATION OF BEAM GAIN

For the sake of analysis, all beams are generated by the uniform linear array (ULA), and the beamwidth is set as the half-power beamwidth (HPBW) [27], i.e.,

$$\Theta_i = 2 \left[\frac{\pi}{2} - \cos^{-1} \left(\frac{1.391\lambda_a}{\pi N_a d_a} \right) \right], i \in \{1, 2, \dots, N_g\}, \quad (17)$$

where λ_a represents the wavelength, d_a represents the spacing of array elements, N_a represents the number of array elements, and $d_a/\lambda_a = 1/4$. Then, the number of array elements required to generate the beam with the beamwidth in (17) can be calculated by

$$N_a = \left\lceil \frac{1.391\lambda_a}{\pi d_a \cos \left(\frac{\pi}{2} - \frac{\Theta_i}{2} \right)} \right\rceil. \quad (18)$$

Finally, the gain of the beam is given by

$$f_i(\theta) = \frac{\sin \left\{ \frac{N_a}{2} [kd_a \cos(\theta - \phi_i) + \beta] \right\}}{N_a \sin \left\{ \frac{1}{2} [kd_a \cos(\theta - \phi_i) + \beta] \right\}}, \quad (19)$$

where k is equal to $2\pi/\lambda_a$, and β represents the phase difference between array elements. The maximum gain of the beam is set to be 1 for the sake of normalization, namely $\max f_i(\theta) = 1$.

REFERENCES

- [1] N. Varsier, L.-A. Dufrene, M. Dumay, Q. Lampin, and J. Schwoerer, "A 5G new radio for balanced and mixed IoT use cases: Challenges and key enablers in FR1 band," *IEEE Commun. Mag.*, vol. 59, no. 4, pp. 82–87, Apr. 2021.
- [2] H. Tataria, M. Shafi, M. Dohler, and S. Sun, "Six critical challenges for 6G wireless systems: A summary and some solutions," *IEEE Veh. Technol. Mag.*, vol. 17, no. 1, pp. 16–26, Mar. 2022.
- [3] M. El-Tanab and W. Hamouda, "An overview of uplink access techniques in machine-type communications," *IEEE Netw.*, vol. 35, no. 3, pp. 246–251, May/Jun. 2022.
- [4] A. Laya, L. Alonso, and J. Alonso-Zarate, "Is the random access channel of LTE and LTE-A suitable for M2M communications? A survey of alternatives," *IEEE Commun. Surveys Tuts.*, vol. 16, no. 1, pp. 4–16, Firstquarter 2014.
- [5] F. Ghavimi and H.-H. Chen, "M2M communications in 3GPP LTE/LTE-A networks: Architectures, service requirements, challenges, and applications," *IEEE Commun. Surveys Tuts.*, vol. 17, no. 2, pp. 525–549, Secondquarter 2015.
- [6] "Study on RAN improvements for machine-type communications," 3GPP TR 37.868 v11.0.0, Sep. 2011.
- [7] S.-Y. Lien, T.-H. Liao, C.-Y. Kao, and K.-C. Chen, "Cooperative access class barring for machine-to-machine communications," *IEEE Trans. Wireless Commun.*, vol. 11, no. 1, pp. 27–32, Jan. 2012.
- [8] Z. Wang and V. W. S. Wong, "Optimal access class barring for stationary machine type communication devices with timing advance information," *IEEE Trans. Wireless Commun.*, vol. 14, no. 10, pp. 5374–5387, Oct. 2015.
- [9] S. Duan, V. Shah-Mansouri, Z. Wang, and V. W. S. Wong, "D-ACB: Adaptive congestion control algorithm for bursty M2M traffic in LTE networks," *IEEE Trans. Veh. Technol.*, vol. 65, no. 12, pp. 9847–9861, Dec. 2016.
- [10] H. Jin, W. T. Toor, B. C. Jung, and J.-B. Seo, "Recursive pseudo-bayesian access class barring for M2M communications in LTE systems," *IEEE Trans. Veh. Technol.*, vol. 66, no. 9, pp. 8595–8599, Sep. 2017.
- [11] X. Yang, A. Fapojuwo, and E. Egbogah, "Performance analysis and parameter optimization of random access backoff algorithm in LTE," in *Proc. IEEE Vehicular Technology Conference (VTC Fall)*, Quebec City, QC, Canada, Sep. 2012, pp. 1–5.
- [12] J. Chen, R.-G. Cheng, O. Agbodike, and Y.-S. Lyu, "A dynamic backoff window scheme for machine-type communications in cyber-physical systems," *IEEE Access*, vol. 8, pp. 31 045–31 056, Feb. 2020.
- [13] H. D. Althumali, M. Othman, N. K. Noordin, and Z. M. Hanapi, "Dynamic backoff collision resolution for massive M2M random access in cellular IoT networks," *IEEE Access*, vol. 8, pp. 201 345–201 359, Nov. 2020.
- [14] W. Li, Q. Du, L. Liu, P. Ren, Y. Wang, and L. Sun, "Dynamic allocation of rach resource for clustered M2M communications in LTE networks," in *Proc. International Conference on Identification, Information, and Knowledge in the Internet of Things (IIKI)*, Beijing, China, Oct. 2015, pp. 140–145.
- [15] H.-Y. Hwang, S.-M. Oh, C. Lee, J. H. Kim, and J. Shin, "Dynamic RACH preamble allocation scheme," in *Proc. International Conference on Information and Communication Technology Convergence (ICTC)*, Jeju Island, South Korea, Oct. 2015, pp. 770–772.
- [16] N. Shahin, R. Ali, and Y.-T. Kim, "Hybrid slotted-CSMA/CA-TDMA for efficient massive registration of IoT devices," *IEEE Access*, vol. 6, pp. 18 366–18 382, Mar. 2018.
- [17] N. K. Pratas, H. Thomsen, C. Stefanovic, and P. Popovski, "Code-expanded random access for machine-type communications," in *Proc. IEEE Globecom Workshops*, Anaheim, CA, USA, Dec. 2012, pp. 1681–1686.
- [18] J. S. Kim, S. Lee, and M. Y. Chung, "Efficient random-access scheme for massive connectivity in 3GPP low-cost machine-type communications," *IEEE Trans. Veh. Technol.*, vol. 66, no. 7, pp. 6280–6290, Jul. 2017.
- [19] L. Liu and W. Yu, "Massive connectivity with massive MIMO—Part I: Device activity detection and channel estimation," *IEEE Trans. Signal Process.*, vol. 66, no. 11, pp. 2933–2946, Jun. 2018.

- [20] H. Han, Y. Li, W. Zhai, and L. Qian, "A grant-free random access scheme for M2M communication in massive MIMO systems," *IEEE Trans. Signal Process.*, vol. 7, no. 4, pp. 3602–3613, Apr. 2020.
- [21] F. Rusek, D. Persson, Buon Kiong Lau, E. G. Larsson, T. L. Marzetta, and F. Tufvesson, "Scaling up MIMO: Opportunities and challenges with very large arrays," *IEEE Signal Process. Mag.*, vol. 30, no. 1, pp. 40–60, Jan. 2013.
- [22] E. G. Larsson, O. Edfors, F. Tufvesson, and T. L. Marzetta, "Massive MIMO for next generation wireless systems," *IEEE Commun. Mag.*, vol. 52, no. 2, pp. 186–195, Feb. 2014.
- [23] X. Xiong, L. Hou, and L. Zhao, "A group-based massive multiple access scheme in cellular M2M networks," *Elsevier Computer Communications*, vol. 121, pp. 44–49, May 2018.
- [24] E. d. Carvalho, E. Bjornson, J. H. Sorensen, P. Popovski, and E. G. Larsson, "Random access protocols for massive MIMO," *IEEE Commun. Mag.*, vol. 55, no. 5, pp. 216–222, May 2017.
- [25] R. S. Sutton and A. G. Barto, *Reinforcement Learning: An Introduction (2nd Edition)*. Cambridge, MA: MIT Press, 2018.
- [26] H. v. Hasselt, A. Guez, and D. Silver, "Deep reinforcement learning with double Q-learning," in *Proc. AAAI Conference on Artificial Intelligence*, Phoenix, AZ, USA, Feb. 2016, pp. 2094–2100.
- [27] C. A. Balanis, *Antenna Theory: Analysis and Design (4th Edition)*. Hoboken, NJ: Wiley, 2016.